

Reaction mechanism and kinetics of DEET visible light assisted photocatalytic ozonation with WO₃ catalyst



Estefanía Mena, Ana Rey*, Eva M. Rodríguez, Fernando J. Beltrán

Departamento de Ingeniería Química y Química Física, Universidad de Extremadura, Av. Elvas s/n, 06006 Badajoz, Spain

ARTICLE INFO

Article history:

Received 27 May 2016

Received in revised form 2 September 2016

Accepted 13 September 2016

Available online 15 September 2016

Keywords:

Photocatalytic ozonation

DEET

WO₃

Mechanism

Kinetics

ABSTRACT

This work is focused on the mechanistic investigation of *N,N*-diethyl-*meta*-toluamide (DEET) degradation by photocatalytic ozonation, using WO₃ in suspension and visible radiation (wavelength ≥ 390 nm). This combined process proved to be an efficient treatment to completely remove the contaminant, HO• radicals being the main species involved. Different oxidation products were identified by liquid chromatography time-of-flight mass spectrometry and ion chromatography analyses, and the evolution of their relative abundances with reaction time was established. The efficiency of photocatalytic ozonation treatment was pointed out not only in the DEET depletion rate but also in the evolution of the main intermediate species and mineralization. All the large intermediates initially formed were completely removed within 60 min reaction time and only short-chain organic acids with very low toxicity remained in solution at concentrations in agreement with the mineralization degree achieved (up to 60% in 2 h). A reaction mechanism of photocatalytic ozonation of DEET involving different chemical reaction steps, with the final formation of short-chain organic acids and mineralization to CO₂, has been proposed. A lumped kinetic model based on TOC and hydroxyl radical reaction was developed to simulate DEET, intermediates and short-chain organic acids evolution in terms of TOC that provides a simplified approach for this process.

© 2016 Elsevier B.V. All rights reserved.

1. Introduction

Pharmaceutical and Personal Care Products (PPCPs) are emerging contaminants of increasing environmental concern due to their continuous discharge into the aquatic environment, persistence and toxic effect in human and wildlife health. Among them, *N,N*-diethyl-*meta*-toluamide (DEET) has been widely used as the active compound in insect repellents for protection against mosquito [1]. Due to its extensive use, in the last few years DEET has been detected in different aquatic systems, wastewater treatment plant effluents and even in drinking water treated, thus indicating its recalcitrance to conventional treatments [2,3]. Although DEET is considered to be slightly toxic to aquatic invertebrates and freshwater fish [2], it has been reported to have potential carcinogenic properties in human nasal mucosal cells [4]. In addition, ingestion of low doses of DEET in children has been reported to result in coma and seizures [5]. Therefore, it is critical to develop a fundamental understanding of the fate and degradation of DEET during water treatment processes.

DEET degradation through different ozone-based processes like ozonation [4], ozone combined with hydrogen peroxide and/or UV radiation [6], and photocatalytic treatments has been studied [1,3,6–8], the last being the most efficient whereas single ozonation resulted to be ineffective for being so slow. However, the combination of ozone and heterogeneous photocatalysis (photocatalytic ozonation), has demonstrated to lead to higher mineralization rates compared to the individual treatments, due to the generation of higher concentration of oxidizing species, mainly hydroxyl radicals, and also the inhibition of e^-/h^+ pair recombination to some extent [9,10]. Photocatalytic ozonation of DEET has been previously investigated using TiO₂ as photocatalyst and UV ($\lambda = 254$ nm) as radiation source [6]. For the practical deployment of photocatalytic technologies, the use of natural solar radiation would be an advantage. In this line, to improve the efficiency of the process, in a previous work photocatalytic ozonation of DEET was studied using different forms of WO₃, a visible-light-responsive semiconductor. According to this work, a monoclinic WO₃ catalyst with W reduced states gave rise to complete DEET removal and high mineralization degree in less than 2 h [11].

However, it is known that the degradation of DEET during ozonation or photocatalytic oxidation proceeds through complex redox reactions involving different steps which can lead to the formation of different intermediates (from now on transforma-

* Corresponding author.

E-mail addresses: emenarub@alumnos.unex.es (E. Mena), anarey@unex.es (A. Rey), evarguez@unex.es (E.M. Rodríguez), fbeltran@unex.es (F.J. Beltrán).

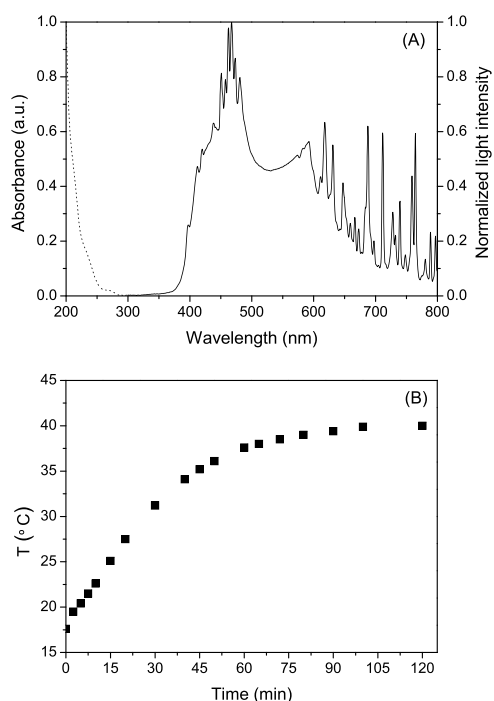


Fig. 1. (A) Spectral irradiance of Xe light after passing through the polyester filter (line) and absorption spectra of DEET (dotted line). (B) Evolution of the temperature of the reaction media with time at the experimental conditions applied in this work.

tion products, TPs) if complete mineralization is not achieved [1,4]. Some of these TPs can be toxic and, in some cases, more persistent than the parent compound [1]. Thus, the identification of these TPs and their reactivity is a key step in optimizing the processes conditions in order to increase their efficiency.

To the best of our knowledge, although there are studies dealing with the identification of TPs generated from DEET during ozonation [4,12] and heterogeneous photocatalysis with TiO_2 [1,8], there are no works focused on the identification of DEET photocatalytic ozonation TPs. Thus, the purpose of this work is to study the visible light assisted photocatalytic ozonation of DEET using WO_3 as catalyst with special interest in 1) identification of DEET TPs and other intermediates; 2) determination of main species involved in DEET degradation with the aid of different scavengers; and 3) development of a kinetic model for the process based on the previous results.

2. Experimental section

2.1. Experiments

All the experiments were carried out in semi-batch mode in a 0.5 L effective volume glass-made spherical reactor, provided with gas inlet, gas outlet and liquid sampling port. The reactor was placed in the chamber of a solar simulator (Suntest CPS, Atlas) provided with a 1500 W Xe lamp with emission restricted to wavelengths above 390 nm using a polyester cut-off filter (Edmund Optics). The spectral irradiance of incident radiation shown in Fig. 1(A), was measured with a spectral-radiometer Black Comet C (StellarNet), provided with an optic fibre for the wavelength range between 190 and 850 nm. The irradiation intensity was set at 550 W m^{-2} and the temperature increased from 20 to 40°C throughout the experiments. A typical temperature vs time profile is shown in Fig. 1(B). An ozone generator (Anseros Ozomat Com AD-02) was used to produce a gaseous ozone-oxygen stream that was fed to the reactor.

In a typical ozonation experiment, the reactor was loaded with 0.5 L of an aqueous solution containing 15 mg L^{-1} of DEET ($\text{pH}_0 = 6$) and covered with aluminium foil when needed (experiments in the dark). Then, the Xe lamp was switched on and at the same time an ozone-oxygen mixture (10 mg L^{-1} ozone concentration) was fed to the reactor at a flow rate of 15 L h^{-1} . Photolysis and photocatalytic oxidation of DEET were also performed in absence of ozone. For catalytic and photocatalytic experiments the same procedure was followed but 0.125 g of the catalyst was added and the suspension was stirred for 30 min before switching on the lamp and/or opening the gas flow (O_2 or O_2/O_3), in order to attain the adsorption equilibrium. The catalyst used was a monoclinic WO_3 -microspheres sample synthesized by sol-gel procedure and calcined at 600°C as reported in a previous work [11]. Adsorption of DEET onto the catalyst was also tested in absence of ozone in the dark.

On the other hand, in some experiments, appropriate amounts of scavengers (*tert*-butyl alcohol (t-BuOH) and oxalate) were added to the DEET aqueous solution in order to determine the nature of the main species involved in DEET degradation. An additional experiment of photocatalytic ozonation of *p*-chlorobenzoic acid (pCBA, 5 mg L^{-1}) in the presence of oxalic acid (0.01 M) was carried out at similar operating conditions for kinetics considerations. In all cases the time for each oxidation experiment was 2 h. At different intervals samples were withdrawn from the reactor and filtered through a $0.2 \mu\text{m}$ PET membrane.

2.2. Analytical methods

DEET concentration was analyzed by HPLC-DAD (Hitachi, Elite LaChrom) using a Phenomenex C-18 column ($5 \mu\text{m}$, 150 mm long and 3 mm diameter) as stationary phase and 0.6 mL min^{-1} of acetonitrile-acidified water (0.1% formic acid) as mobile phase (30–70 v/v, isocratic). Identification and quantification was carried out at 220 nm. The concentration of pCBA was analysed in the same system with the same column and mobile phase at 0.7 mL min^{-1} , and its identification and quantification was carried out at 238 nm. Total organic carbon (TOC) was measured using a Shimadzu TOC-VSCH analyzer. Aqueous ozone concentration was measured by the indigo method using an UV-vis spectrophotometer (Evolution 201, Thermospectronic) set at 600 nm [13]. In this assay, 3 mL of sample were mixed with 3 mL of indigo solution and then filtered to remove catalyst particles. Spectrophotometric measurements were immediately carried out to avoid possible interferences [14]. Concentration of ozone in the gas phase was continuously monitored by means of an Anseros Ozomat GM-6000 Pro analyzer. Hydrogen peroxide concentration was determined photometrically by the cobalt/bicarbonate method, at 260 nm using the same UV-vis spectrophotometer [15].

DEET organic TPs were identified by HPLC-qTOF using an Agilent 6530 accurate mass quadrupole time-of-flight mass spectrometer bearing with electrospray ionization (ESI) source coupled with Agilent 1260 series LC system. A ZORBAX SB-C18 column ($3.5 \mu\text{m}$, 150 mm long, and 4.6 mm diameter) was used as stationary phase. The column was kept at constant temperature of 30°C during each analysis. As mobile phase, 0.2 mL min^{-1} of acetonitrile-acidified water (25 mM formic acid) was used from 10 to 100% of acetonitrile in 40 min with 15 min of equilibration. The injection volume was $10 \mu\text{L}$. The qTOF instrument was operated in the 4 GHz high-resolution mode. Ions are generated using an electrospray ion source Dual ESI. Electrospray conditions were the following: capillary, 3500 V; nebulizer, 30 psi; drying gas, 10 L min^{-1} ; gas temperature, 350°C ; skimmer voltage, 65 V; octapole RF peak, 750 V; fragmentor, 175 V. The mass axis was calibrated using the mixture provided by the manufacturer over the m/z 70–3200 range. A sprayer with a reference solution was used as continuous calibration in positive ion using the following reference masses: m/z

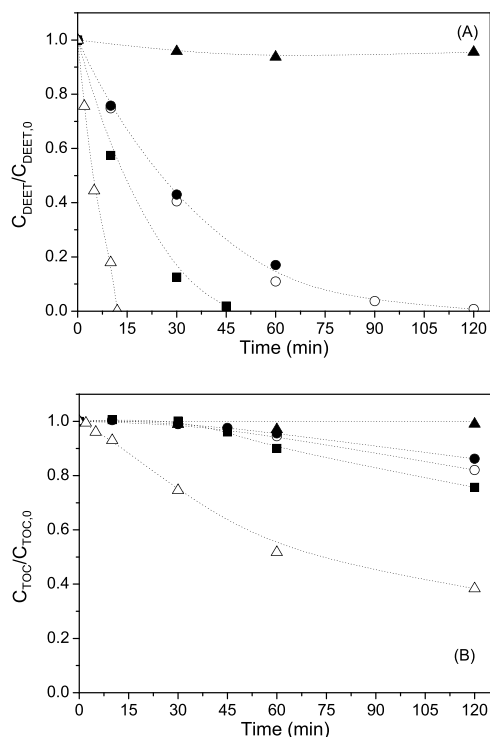


Fig. 2. Evolution of DEET (A) and TOC (B) normalized concentration with time during the different treatments applied: \blacktriangle PhC-O₂; \circ O₃; \blacksquare Ph-O₃; \bullet C-O₃; \triangle PhC-O₃. Experimental conditions: $C_{DEET,0} = 15 \text{ mg L}^{-1}$; $\text{pH}_0 = 6$; $V = 0.5 \text{ L}$; $Q_g = 15 \text{ L h}^{-1}$; $^*C_{O_3,g} = 10 \text{ mg L}^{-1}$; $^*I = 550 \text{ W m}^{-2}$; $^*C_{WO_3} = 0.25 \text{ g L}^{-1}$ (*if applied).

121.0509 and 922.0098. Data were processed using Agilent Mass Hunter Workstation Software (version B.04.00).

According to previous works, the generation of formaldehyde during DEET degradation is expected [1,8]. Thus, concentration of formaldehyde in solution was measured by Hantzsch reaction, measuring the absorbance at 412 nm of the diacetyldihydrolutidine formed [16]. Finally, short-chain organic acids and inorganic ions were analyzed by an Ion Chromatograph with chemical suppression (Metrohm 881 Compact Pro) provided with a conductivity detector using a MetroSep A sup 5 column (250 mm long, 4 mm diameter) at 45°C and 0.7 mL min^{-1} of Na_2CO_3 from 0.6–14.6 mM in 50 min (10 min post-time for equilibration) as mobile phase.

3. Results and discussion

3.1. Comparison of processes

In a first series of experiments, the effectiveness of adsorption, photolysis under $\lambda \geq 390 \text{ nm}$ (Ph), ozonation (O₃), photolytic ozonation (Ph-O₃), photocatalytic oxidation (PhC-O₂), catalytic ozonation (C-O₃) and photocatalytic ozonation (PhC-O₃) on DEET removal was studied. On the one hand, from the obtained results (not shown) it is deduced that contribution of both adsorption onto the catalyst and direct photolysis to DEET removal is negligible, the latter as expected since there is not overlapping between DEET absorption and lamp emission spectra, as deduced from Fig. 1(A). On the other hand, time-evolution of normalized DEET and TOC concentration for the different processes studied is shown in Fig. 2(A) and Fig. 2(B), respectively. According to these figures, degradation rate of DEET during photocatalytic oxidation (PhC-O₂) was very low. Thus, less than 10% of DEET conversion was attained after 120 min and no mineralization was observed. Taking into account that WO₃ is a visible light responsive semiconductor, these poor results could be attributable to the fact that oxygen is not

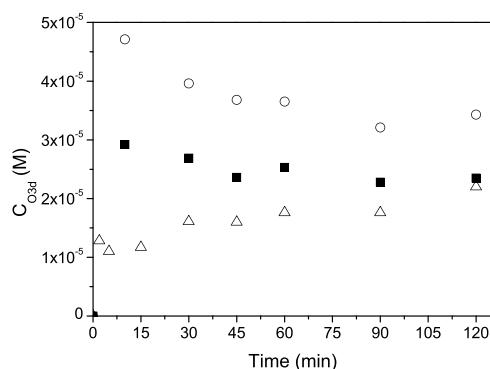


Fig. 3. Evolution of dissolved ozone concentration with time during the application of different processes. Symbols: \circ O₃; \blacksquare Ph-O₃; \triangle PhC-O₃. Experimental conditions: $C_{DEET,0} = 15 \text{ mg L}^{-1}$; $\text{pH}_0 = 6$; $V = 0.5 \text{ L}$; $Q_g = 15 \text{ L h}^{-1}$; $C_{O_3,g} = 10 \text{ mg L}^{-1}$; $^*I = 550 \text{ W m}^{-2}$; $^*C_{WO_3} = 0.25 \text{ g L}^{-1}$ (*if applied).

able to react with photoexcited electrons in the conduction band of WO₃ [17], leading to a high recombination rate of e^-/h^+ pairs and, as a consequence, presenting a low efficiency in the photocatalytic oxidation process.

Regarding single ozonation (O₃), at the conditions tested the conversion of DEET after 2 h was 100% as shown in Fig. 2(A). Given the low reactivity of ozone towards DEET ($k_{O_3} = 0.123 \text{ M}^{-1} \text{ s}^{-1}$ at 20°C [4]), the results suggest the participation of ozone indirect reactions, namely hydroxyl radical generation from O₃ decomposition, on the elimination of the contaminant. Besides, the relatively low TOC removal achieved ($\sim 20\%$ after 2 h, see Fig. 2(B)) could be related to the formation of intermediates refractory to ozone direct reaction [18]. All these aspects are discussed in depth in subsequent sections.

From Fig. 2 it can also be seen that addition of WO₃ catalyst (C-O₃ system) had no effect on the effectiveness of the ozonation in terms of DEET and TOC removal, which indicates the inability of the catalyst to promote an efficient O₃ decomposition in the dark.

On the other hand, when light ($\lambda \geq 390 \text{ nm}$) and ozone were combined (Ph-O₃), DEET degradation rate was higher than the observed for the O₃ system in the dark. In this sense, from Fig. 2(A) it is deduced that the time needed to reach a given DEET conversion by Ph-O₃ was almost half the time needed in the dark. Besides, in line with the above the mineralization was also higher (Fig. 2(B)), reaching a TOC removal of 18% and 25% in absence and presence of light, respectively, after 2 h of treatment. Since the direct photolysis of the pollutant does not occur, the increased efficiency of the Ph-O₃ system compared to O₃ should be related to the interaction between ozone and light leading to the formation of reactive species as has been previously reported [19,20].

Undoubtedly, addition of WO₃ to the Ph-O₃ system, that is, photocatalytic ozonation (PhC-O₃) led to the best results among the processes tested. As observed in Fig. 2, after 15 min DEET was completely removed and the mineralization degree was higher than 60% after 2 h. These results suggest that, unlike oxygen, recombination of e^-/h^+ generated from WO₃ photoexcitation is avoided thanks to ozone electron trapping [17]. On its role as an electron acceptor ozone would decompose into reactive oxygen species (mainly HO \cdot) thus increasing the degradation and mineralization rate of the pollutant. These results are consistent with the evolution of dissolved ozone shown in Fig. 3. As observed, in the presence of light the concentration of ozone in solution diminishes and more markedly when WO₃ is also present. Therefore, it seems that both light ($\lambda \geq 390 \text{ nm}$) and WO₃ + light promotes ozone decomposition which, in turn, leads to the formation of highly reactive species that would be responsible for the faster elimination rate of DEET and TOC observed. Another aspect to highlight from Fig. 3 is the time

Table 1

Second-order rate constants for the reaction of ozone and hydroxyl radicals with DEET, t-BuOH, oxalate and p-CBA.

Compound	k_{O_3} ($M^{-1} s^{-1}$)	Refs.	k_{HO} ($M^{-1} s^{-1}$)	Refs.
DEET	20 °C: 0.121 ± 0.005 Conditions: pH = 2–9; $C_{DEET,0} = 10^{-6}$ M; $C_{t-BuOH,0} = 0.1$ M 15 °C: 2.46 ± 0.09 ($R^2 = 0.991$) 25 °C: 4.24 ± 0.17 ($R^2 = 0.985$) 40 °C: 7.05 ± 0.33 ($R^2 = 0.987$) $k_{O_3} = Ae^{-E_a/RT}$; $A = 1.2 \times 10^6 M^{-1} s^{-1}$; $E_a = 31.3 kJ mol^{-1}$ ($R^2 = 0.988$) Conditions: pH = 2, $C_{DEET,0} = 4 \times 10^{-5}$ M; $C_{t-BuOH,0} = 0.004$ M	[4] This work	4.95×10^9	[21]
t-BuOH	0.0011	[22]	6.2×10^8	[23]
Oxalate	<0.04	[30]	5×10^7 (pH = 2.8) 7.7×10^6 (pH = 6)	[31]
p-CBA	≤ 0.015	[39]	5×10^9	[39]

profile of dissolved ozone (O_{3d}) concentration during single ozonation. As observed, it reaches a maximum at the beginning of the experiment and then decreases gradually until reaching a stationary value. This behavior differs from that usually observed during ozonation of water solutions where O_{3d} concentration is low at the beginning and gradually increases reaching the stationary value. The explanation to this fact lies in the temperature profile inside the reactor shown in Fig. 1(B). During the first 60 min, as the temperature increases from ~20 °C to 40 °C ozone solubility decreases. From that moment, since the temperature remains almost constant a stationary value of ozone in solution is also maintained. In addition to ozone solubility, temperature can also affect the kinetics of ozone reactions whereas its effect on the reactivity of transient species is much lower. With this in mind, the rate constant of the direct reaction between DEET and ozone at 15 °C, 25 °C and 40 °C has been determined by a direct method [18]. Taking into account the low k_{O_3} values expected according to the literature ($0.123 M^{-1} s^{-1}$ at 20 °C, [4]), and the fact that DEET does not dissociate in water, the study was performed at pH = 2 (pH adjustment with perchloric acid) in a thermostated bubble column (reaction volume 250 mL) operating under semibatch-mode by continuous injection of $15 L h^{-1}$ of a gaseous mixture containing $10 mg L^{-1}$ of O_3 . In these experiments t-BuOH was used as scavenger of HO^\bullet radicals that could be generated from O_3 decomposition. According to the second-order rate constants values reported in the literature (see Table 1) for the reaction of both compounds with O_3 and HO^\bullet [4,21–23], the initial concentration of DEET and t-BuOH was set at 4×10^{-5} M and 4×10^{-3} M, respectively. At these conditions, according to Table 1 reaction of DEET with HO^\bullet will be avoided whereas t-BuOH will not be able to compete with DEET for ozone. Also, the experimental conditions aimed to allow DEET and ozone to react in the liquid bulk (i.e., slow kinetic regime of ozone absorption) were established so that the DEET mass balance in the semicontinuous perfectly mixed reactor used would be given by Eq. (1):

$$-\frac{dC_{DEET}}{dt} = \frac{k_{O_3-DEET}}{Z_{DEET}} C_{O_{3d}} C_{DEET} \quad (1)$$

where $C_{O_{3d}}$ and C_{DEET} are the concentration of ozone and DEET in the liquid, respectively, and Z_{DEET} the stoichiometry of the reaction between O_3 and DEET, which was considered to be 1 mol of O_3 consumed per mol of DEET according to its low reactivity and the structure of DEET molecule. Integration of Eq. (1) leads to Eq. (2) which, in case $C_{O_{3d}}$ remains constant, simplifies to Eq. (3):

$$\ln \frac{C_{DEET0}}{C_{DEET}} = k_{O_3-DEET} \int_{t_0}^t C_{O_{3d}} dt \quad (2)$$

$$\ln \frac{C_{DEET0}}{C_{DEET}} = k_{O_3-DEET} C_{O_{3d}} t \quad (3)$$

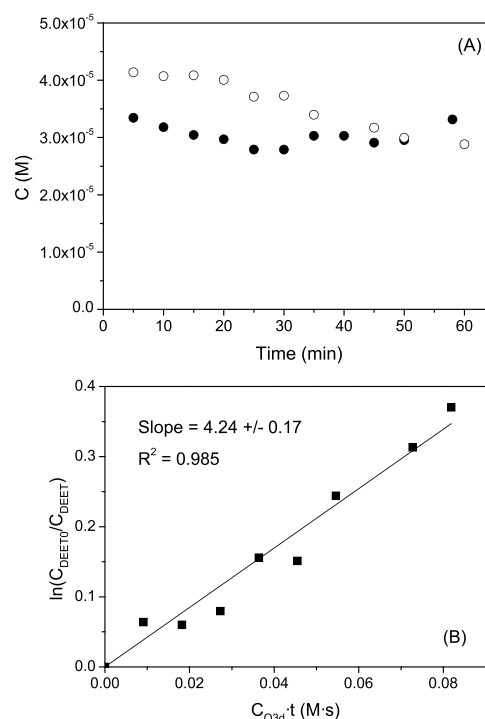


Fig. 4. Determination k_{O_3-DEET} at 25 °C. (A) Evolution of DEET (○) and O_{3d} (●) concentration with time. (B) Fitting of data to Eq. (3). Experimental conditions: $C_{DEET,0} = 10 mg L^{-1}$; $C_{t-BuOH} = 0.004 mol L^{-1}$; $pH_0 = 2$; $V = 0.25 L$; $Q_g = 15 L h^{-1}$; $C_{O_3,g} = 10 mg L^{-1}$.

According to Eq. (3), a plot of the left term against ($C_{O_{3d}}t$) should lead to a straight line that intercepts the origin and whose slope is the value of k_{O_3-DEET} . As an example, in Fig. 4 the results obtained at 25 °C are shown. As observed in Fig. 4(A) during the run $C_{O_{3d}}$ was practically constant from $t = 5$ min ($C_{O_{3d}} = (3.03 \pm 0.18) \times 10^{-5}$ M). On the other hand, from experimental data fitting to Eq. (3) (shown in Fig. 4(B)) a k_{O_3-DEET} value of $4.24 \pm 0.17 M^{-1} s^{-1}$ ($R^2 = 0.985$) was obtained at 25 °C. Following a similar procedure, k_{O_3-DEET} values of $2.46 \pm 0.09 M^{-1} s^{-1}$ and $7.05 \pm 0.33 M^{-1} s^{-1}$ were obtained at 15 °C and 40 °C, respectively. To validate these rate constant values, the slow kinetic regime of ozone absorption (Hatta number, $Ha < 0.3$, [18]) was verified taking into account Eq. (4):

$$Ha = \frac{\sqrt{k_{O_3-DEET} C_{DEET} D_{O_3}}}{k_l} \quad (4)$$

where D_{O_3} is the diffusivity of ozone in water ($1.76 \times 10^{-9} m^2 s^{-1}$; [24]); and k_l the individual liquid-side mass transfer coefficient calculated to be $3.74 \times 10^{-4} m s^{-1}$ by applying the Calderbank's

Equation [25]. At the conditions applied in this work Ha was always much lower than 0.3, allowing us to validate the k_{O_3-DEET} values summarized in Table 1. As deduced from Table 1, although in all cases the low reactivity of ozone towards DEET is highlighted, k_{O_3-DEET} values obtained in this work are considerable greater than that reported by Benítez et al. [4]. This could be attributable to the low $C_{DEET,0}/C_{t-BuOH,0}$ ratio applied by these authors at which the alcohol acts as both HO^\bullet and ozone scavenger. Finally, the k_{O_3-DEET} values obtained at different temperatures were fitted to the Arrhenius equation. The pre-exponential factor and the activation energy are also indicated in Table 1.

3.2. Determination of the main species responsible for DEET degradation and mineralization

In order to determine the nature of the species involved on the elimination of DEET through the most effective systems, namely ozonation, photolytic ozonation and photocatalytic ozonation, a new series of experiments was carried out by adding substances capable of acting as scavengers of some of the species whose generation and participation is expected. In this sense, *t*-BuOH has been selected as scavenger of HO^\bullet in the liquid bulk, and oxalate as scavenger of HO^\bullet both in the liquid bulk and also at the catalyst surface where, in addition, adsorbed oxalate can be oxidized by the photogenerated positive holes (h^+) [26–29]. As commented in the previous section, to select the appropriate substances to be used as scavengers their reactivity towards the different species and reagents involved must be firstly considered. Thus, in Table 1 the rate constant of the reactions oxalate-ozone and oxalate- HO^\bullet are also indicated [30,31]. Taking into account the reactivity of DEET and the scavengers towards the different species involved, this study was carried out at the following conditions: $pH_0 = 6$; $17\text{--}40^\circ\text{C}$ (see Fig. 1(B)); $C_{DEET,0} = 8 \times 10^{-5}\text{ M}$; $C_{Oxal,0} = 10^{-3}\text{ M}$ and/or $C_{t-BuOH,0} = 0.03\text{ M}$. Fig. 5 shows the influence of the presence/absence of these scavengers in DEET degradation rate by the different processes applied: O_3 (Fig. 5(A)), $Ph-O_3$ (Fig. 5(B)) and $PhC-O_3$ (Fig. 5(C)). The theoretical DEET evolution with time has also been calculated from Eq. (1) considering that DEET was only degraded by direct ozone attack. For this purpose $C_{DEET,0}$ value, the evolution of both CO_{3d} (see Fig. 3) and temperature (Fig. 1(B)) with time as well as the influence of T on k_{O_3-DEET} according to Arrhenius equation (see Table 1) have been taken into account. These results have also been added to Fig. 5 for comparative reasons.

Fig. 5(A) shows the effect of the presence of 0.03 M *t*-BuOH in $8 \times 10^{-5}\text{ M}$ DEET elimination rate by single ozonation. At these conditions, *t*-BuOH will react with all HO^\bullet whereas its reaction with O_3 will be negligible. As observed in Fig. 5(A), the presence of *t*-BuOH negatively affect the elimination rate of the contaminant, thus indicating not only the decomposition of ozone into HO^\bullet radicals at the conditions tested but also the high contribution of HO^\bullet to DEET degradation by single ozonation. Moreover, the good agreement between C_{DEET} evolution when *t*-BuOH was present and that calculated by Eq. (1) indicates that O_3 and HO^\bullet are the only species involved on DEET degradation by single ozonation.

Similarly, the influence of 0.03 M *t*-BuOH in the degradation of $8 \times 10^{-5}\text{ M}$ DEET by photolytic ozonation is depicted in Fig. 5(B). Again, the presence of *t*-BuOH negatively affects the elimination rate of the contaminant. However, the elimination rate of DEET calculated from Eq. (1) (straight line) is clearly lower than that experimentally determined in the presence of *t*-BuOH. Since it is expected that at the conditions used most of the HO^\bullet was trapped by *t*-BuOH, there must be other species and/or mechanism different than HO^\bullet and O_3 also contributing to DEET degradation. This effect is more marked during the first 45 min and then, the rate of DEET depletion becomes similar (see Fig. 5(B), Eq. (1) and *t*-BuOH experiment). The fact that the positive effect of the presence of light on

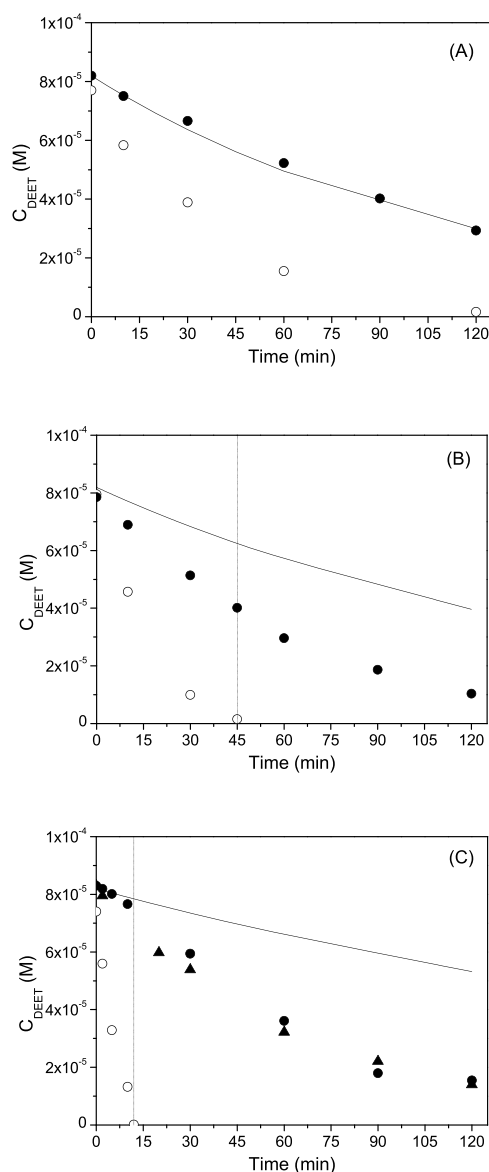


Fig. 5. Influence of the presence of different scavengers on the elimination of DEET by O_3 (A), $Ph-O_3$ (B) and $PhC-O_3$ (C). Symbols: \circ no scavenger; \bullet *t*-BuOH 0.03 M; \blacktriangle *t*-BuOH 0.03 M and Oxalate 10^{-3} M . Line: Calculated from Eq. (1) assuming only direct ozone-DEET reaction. Experimental conditions: $C_{DEET,0} = 15\text{ mg L}^{-1}$; $pH_0 = 6$; $V = 0.5\text{ L}$; $Q_g = 15\text{ L h}^{-1}$; $C_{O_3,g} = 10\text{ mg L}^{-1}$; $I = 550\text{ W m}^{-2}$; $C_{W03} = 0.25\text{ g L}^{-1}$ (*if applied).

TOC removal is much lower than on DEET (Fig. 2), that is, the effect is more noticeable at short reaction times, could indicate the formation of an intermediate capable of acting as a photosensitizer giving rise to the formation of reactive species. Once the intermediate is degraded the beneficial effect of light would disappear.

Finally, the effect of the presence of oxalate and/or *t*-BuOH on the rate of DEET removal by photocatalytic ozonation is shown in Fig. 5(C). It can be observed that the degradation rate of DEET in the presence of *t*-BuOH or *t*-BuOH + oxalate was very similar. Considering that *t*-BuOH only reacts with HO^\bullet in the bulk, these results are pointing out that HO^\bullet and h^+ photogenerated at the catalyst surface do not contribute to DEET degradation. Moreover, it can be observed that 100% DEET removal was attained in less than 15 min by $PhC-O_3$ when no scavengers are used, but the evolution of DEET during the same period when *t*-BuOH was present was virtually coincident with that calculated when only its direct reaction with

ozone is considered (Eq. (1)). Thus, HO^\bullet in the bulk seems to be the only species involved in DEET elimination by PhC-O_3 .

Therefore, as deduced from results in Fig. 5, at the conditions used in this work, during photocatalytic ozonation DEET is mainly removed through its reaction with HO^\bullet radicals in the bulk whose formation when visible radiation, WO_3 catalyst and O_3 are combined (PhC-O_3) is highly enhanced. The highest HO^\bullet concentration would also be the responsible for the highest efficiency of this combination in terms of mineralization (Fig. 2(B)). In other words, the above results confirm that not only DEET but also final products oxidation (mainly carboxylic acids) proceeds through HO^\bullet attack during PhC-O_3 process. Moreover, first TPs degradation is also likely due to HO^\bullet reaction in the bulk as discussed in the following section.

3.3. Identification of TPs

The identification of TPs during ozonation and photocatalytic ozonation was carried out by means of LC-qTOF and ion chromatography. LC-qTOF approach provided accurate mass measurements of ions (m/z values) of the different compounds formed, and several peaks corresponding to equal m/z values. In total, 22 TPs were identified, which are indicated in Table 2 together with the parent compound DEET. They were designated by a number corresponding to the m/z value and for isomers the number is followed by a letter in alphabetical order with increasing retention time. The low experimental relative mass errors obtained indicate the high grade of confidence in the assignment of the elemental composition. In this sense, relative mass errors below 5 ppm are generally accepted for the verification of the elemental composition [32]. Table 2 also includes the tentative structures proposed for the different TPs according to the specific literature [1,4,8,12,21,33,34]. These TPs identified, similar to those found in previous works for different systems, are consistent with the attack of HO^\bullet generated throughout the processes. Although neither the tentative structures nor the concentration of the TPs could be confirmed due to the lack of standards, reaction pathways for DEET degradation have been proposed and are discussed in the following section.

In general, main first intermediates detected were large molecules, such as $\text{C}_{12}\text{H}_{15}\text{NO}_2$ ($m/z=206$), $\text{C}_{12}\text{H}_{17}\text{NO}_2$ ($m/z=208$), $\text{C}_{10}\text{H}_{15}\text{NO}_2$ ($m/z=182$), $\text{C}_{10}\text{H}_{15}\text{NO}_3$ ($m/z=198$) or $\text{C}_{10}\text{H}_{13}\text{NO}$ ($m/z=164$), in which practically the parent compound structure ($\text{C}_{12}\text{H}_{17}\text{NO}$, $m/z=192$) is still present with slight modifications. Other smaller intermediates like $\text{C}_5\text{H}_{11}\text{NO}_2$ ($m/z=118$) or $\text{C}_4\text{H}_{11}\text{N}$ ($m/z=74$) that have been identified are formed after the cleavage of characteristic bonds.

The evolution with time of the intensity of the signal of DEET and those TPs detected by LC-qTOF during O_3 and PhC-O_3 processes is shown in Fig. 6. According to Fig. 6 OPs formed were exactly the same regardless of the process applied although their formation rate was noticeably much faster during the photocatalytic ozonation treatment. Thus, during PhC-O_3 total TPs disappearance was observed at 60 min whereas for single ozonation some of these TPs still remained after 120 min.

As deduced in the previous section, the fact that HO^\bullet radicals in the bulk are the main species involved in DEET degradation by O_3 and PhC-O_3 could explain, on one hand, that TPs formed are the same in both processes and, on the other hand, that TPs formation rate in the photocatalytic treatment presents the highest values as a result of the largest concentration of HO^\bullet in the reaction medium. Moreover, once the maximum concentration of each TP is reached, their removal rate during the PhC-O_3 process is also faster than the observed during O_3 alone process. In summary, during single ozonation direct O_3 reactions are favoured as a consequence of the higher concentration of dissolved molecular ozone and, according to Fig. 6, a higher removal rate of TPs is clearly obtained by PhC-O_3 system. Then, it can be pointed out that, as for DEET, in both

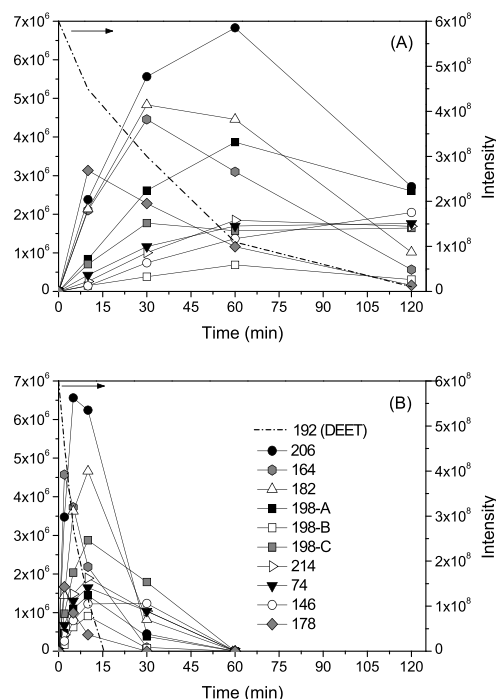


Fig. 6. Time profiles of the intensity of the main peaks detected during (A) O_3 and (B) PhC-O_3 of DEET. Experimental conditions: $C_{\text{DEET},0} = 15 \text{ mg L}^{-1}$; $\text{pH}_0 = 6$; $V = 0.5 \text{ L}$; $Q_g = 15 \text{ L h}^{-1}$; $C_{\text{O}_3,g} = 10 \text{ mg L}^{-1}$; $I = 550 \text{ W m}^{-2}$; $C_{\text{WO}_3} = 0.25 \text{ g L}^{-1}$ (*if applied).

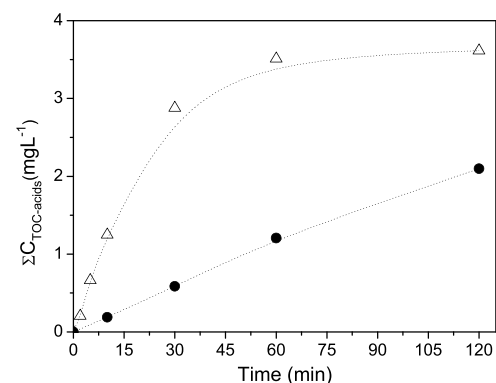


Fig. 7. Evolution of TOC corresponding to short-chain saturated organic acids concentration with time during different processes. Symbols: ● O_3 ; △ PhC-O_3 . Experimental conditions: $C_{\text{DEET},0} = 15 \text{ mg L}^{-1}$; $\text{pH}_0 = 6$; $V = 0.5 \text{ L}$; $Q_g = 15 \text{ L h}^{-1}$; $C_{\text{O}_3,g} = 10 \text{ mg L}^{-1}$; $I = 550 \text{ W m}^{-2}$; $C_{\text{WO}_3} = 0.25 \text{ g L}^{-1}$ (*if applied).

treatments (O_3 and PhC-O_3) the HO^\bullet radical is the main responsible species for the degradation of intermediate TPs.

Further oxidation of these TPs usually gives place to the formation of short-chain saturated carboxylic acids. Thus, the presence of oxalic, acetic, pyruvic and formic acids (see molecular formula and structures in Table 3) was detected at long reaction times for both O_3 and PhC-O_3 processes. In Fig. 7, the evolution with time of C_{TOC} present as carboxylic acids ($\Sigma C_{\text{TOC-acids}}$) is shown. As expected, a higher generation rate and concentration in solution of these acids for PhC-O_3 is observed being 18% and 64% of residual TOC in the form of these organic acids after 2 h of ozonation and photocatalytic ozonation, respectively. By comparing Fig. 6 and Fig. 7, it is deduced that formation of carboxylic acids needs the previous oxidation of TPs, which is faster for photocatalytic ozonation as commented before. Hence, the low TOC conversion into carboxylic acids after 2 h of ozonation indicates that at these conditions intermediate TPs, that could even be more harmful than the parent compound,

Table 2
TPs identified by LC-qTOF during DEET O₃ and PhC-O₃ degradation.

Compound	t _R (min)	Molecular Formula [M]	Experimental m/z [M-H ⁺]	Error (ppm)	Tentative structure [M]
192 (DEET)	24.56	C ₁₂ H ₁₇ NO	192.1385	−2.65	
240-A	16.05	C ₁₂ H ₁₇ NO ₄	240.1234	−10.41	
240-B	16.92		240.1239	−8.32	
240-C	17.4		240.1245	−5.83	
226-A	15.38	C ₁₁ H ₁₅ NO ₄	226.1083	−4.05	
226-B	15.83		226.1085	−4.93	
222-A	18.88	C ₁₂ H ₁₅ NO ₃	222.1128	−3.29	
222-B	20.13		222.1129	−3.85	
214	15.96	C ₁₀ H ₁₅ NO ₄	214.1072	−4.74	
208-A	17.54	C ₁₂ H ₁₇ NO ₂	208.1337	−2.38	
208-B	19.24		208.1339	−3.34	
208-C	20.64		208.1326	2.91	
208-D	21.69		208.1338	−2.86	
206	21.03	C ₁₂ H ₁₅ NO ₂	206.1177	−4.58	
198-A	13.69	C ₁₀ H ₁₅ NO ₃	198.1129	−2.17	
198-B	15.78		198.1129	−2.17	
198-C	16.83		198.1130	−2.68	
182	22.38	C ₁₀ H ₁₅ NO ₂	182.1177	−5.19	
178	22.70	C ₁₁ H ₁₅ NO	178.1229	−1.46	
164	21.48	C ₁₀ H ₁₃ NO	164.1069	−2.50	
146	9.23	C ₆ H ₁₁ NO ₃	146.0812	−2.26	
118	6.55	C ₅ H ₁₁ NO ₂	118.0863	−2.42	
74	6.62	C ₄ H ₁₁ N	74.0967	−6.74	

Table 3
Short-chain saturated organic acids identified during DEET O₃ and PhC–O₃ degradation.

Compound	Molecular Formula	Structure
Oxalic acid	C ₂ H ₂ O ₄	
Acetic acid	C ₂ H ₄ O ₂	
Pyruvic acid	C ₃ H ₄ O ₃	
Formic acid	CH ₂ O ₂	

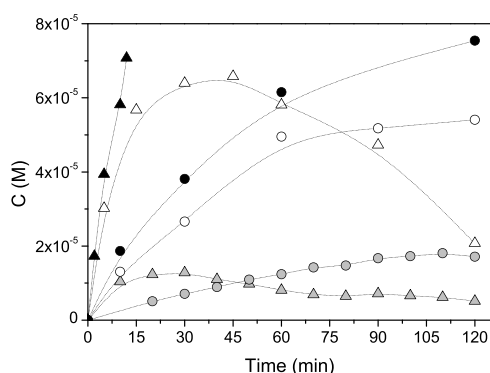


Fig. 8. Evolution of DEET eliminated and H₂O₂ and CH₂O generated with time during DEET degradation by O₃ (circles) and PhC–O₃ (triangles) systems. Symbols: ●, ▲ DEET eliminated; ○, △ H₂O₂ formed; ●, ▲ CH₂O generated. Experimental conditions: C_{DEET,0} = 15 mg L^{−1}; pH₀ = 6; V = 0.5 L; Q_g = 15 L h^{−1}; C_{O₃,g} = 10 mg L^{−1}; I = 550 W m^{−2}; *C_{WO₃} = 0.25 g L^{−1} (*if applied).

are still present. During photocatalytic ozonation, only short-chain organic acids were detected at the end of the treatment, with the complete elimination of the large TPs. Thus, according to the literature [1,4], a significant decrease in the toxicity is expected if this process is applied until reaching a high mineralization degree. However, the information currently available about ecotoxicity is not sufficient and further work would be necessary [2].

According to the literature, ozonation and photocatalytic oxidation of DEET led to the generation of formaldehyde (CH₂O) [1,8]; and also, hydrogen peroxide (H₂O₂) is commonly formed through direct ozone and hydroxyl radical reactions [35,36]. Thus, the evolution of concentration of both compounds with time is depicted in Fig. 8 together with the evolution of DEET eliminated during O₃ and PhC–O₃. It can be clearly seen for both treatments that the disappearance of 1 mol of DEET leads to the formation and accumulation of ~1 mol of H₂O₂ in the reaction medium. Particularly, during PhC–O₃ an increase of H₂O₂ concentration is produced up to 45 min coinciding with the time when TPs were almost completely removed (see Fig. 6(B)). From this moment, H₂O₂ is gradually consumed likely in photocatalytic reactions as discussed in a previous work [11]. However, in case H₂O₂ reactions led to the formation of reactive oxidizing species, they do not seem to participate in TPs removal. In fact, the analysis of H₂O₂ evolution during DEET degradation by the other processes applied in this work, together with the results during photocatalytic oxidation of DEET adding H₂O₂ (PhC–O₂ + H₂O₂, not shown) led us to conclude that: 1) H₂O₂

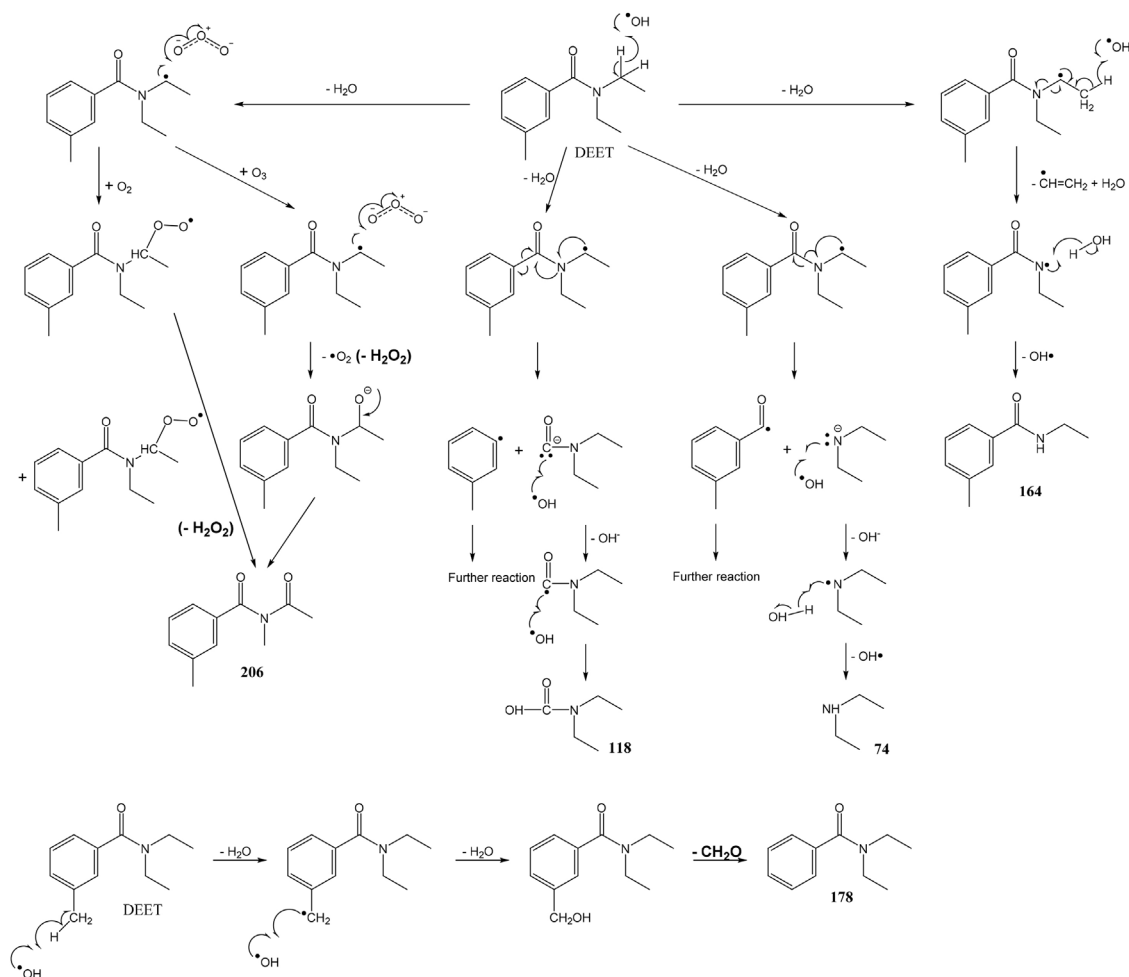
decomposition during the processes applied mainly occurs due to its interaction with the irradiated catalyst surface; and 2) H₂O₂ decomposition does not lead to the generation of reactive species capable of oxidizing DEET and/or its TPs.

Regarding formaldehyde, a direct relation between DEET degradation and formaldehyde formation is also observed although in this case the ratio is ~0.25 mol of CH₂O per mol of DEET eliminated by O₃ and PhC–O₃.

3.4. Proposed reaction mechanism

Bearing in mind the identified TPs and the fact that hydroxyl radical seems to be the main species involved on DEET degradation by PhC–O₃ when WO₃ and light of wavelength higher than 390 nm are used, a tentative mechanism is presented in Schemes 1–3 and discussed below. Both the aliphatic chain and the aromatic ring of DEET molecule are found to react with hydroxyl radicals and pathways will be separately discussed. For the reactions at the aliphatic chain of DEET, the identified TPs and the proposed mechanisms are presented in Scheme 1. In this mechanism, the HO• radical attack on the aliphatic chain could occur by abstraction of hydrogen to form an organic radical in which several TPs are based on [12]. For example, the TP named 206 in Table 2 with *m/z* 206.1177 was generated by a reaction between this organic radical and oxygen or ozone. On the other hand, the rearrangement of the radical formed and an additional HO• attack at the aliphatic chain lead to its de-ethylation to form another radical, which could further react with water to form the TP named 164 (*m/z* 164.1069). Other authors have also reported the existence of these TPs through the above two different pathways during ozonation [4], and photocatalytic oxidation of DEET [1,8]. In addition, the rearrangement of the organic radical could lead to the cleavage of characteristic bonds [12] and subsequent formation of carbanions which could explain the formation of the smaller TPs detected in the present work. On one hand, the rearrangement of the radical produced a new radical in addition to the carbanion of diethylamine. From the HO• radical attack on this carbanion and reaction with water, diethylamine can be formed (TP named 74 in Table 2 with *m/z* 74.0967). On the other hand, the rearrangement of the radical can also form the benzyl radical (involved in further reactions) and a carbanion which could react with HO• radicals to produce hydroxydiethylamide (TP 118 in Table 2 with *m/z* 118.0863). Finally, in Scheme 1 is also considered the initial HO• attack and hydrogen abstraction on the methyl group that is directly attached to the aromatic ring of DEET. The TP 178 with *m/z* 178.1229 is derived by detachment of this methyl group from DEET [1,8], through loss of formaldehyde after a new HO• radical attack.

Regarding the reactions on the aromatic ring of DEET (see Scheme 2), the initial attack of the hydroxyl radical could lead to the generation of hydroxylated DEET derivatives. Thus, in the present study four isomers have been identified for monohydroxy DEET (208-A,B,C,D in Table 2 with *m/z* 208.1326–208.1339) corresponding to the different positions that can be occupied by the HO moiety in the aromatic ring, as it has been reported for the degradation of DEET by anodic Fenton, photolytic processes or photocatalytic treatments [8,21,33,34]. Monohydroxy DEET further reacts with HO• to form dihydroxylated and trihydroxylated DEET. In this sense, three different isomers of trihydroxy DEET have been detected (240-A,B,C in Table 2 with *m/z* 240.1234–240.1245). In addition, hydroxylated derivatives of DEET degradation products were detected. For example, the isomers 222-A,B in Table 2 with *m/z* 222.1128–222.1129 could be formed either by hydroxylation of the 206 TP, or from isomers 208-A,B,C,D through oxidation of the aliphatic chain. In the same way, the isomers 226-A,B (*m/z* 226.1083–226.1085) can be generated by hydroxylation of the 178 TP and also from isomers 240-A,B,C by cleavage of the C–C bond and subsequent detachment of the methyl group from the aro-



Scheme 1. Proposed DEET degradation pathway through HO^\bullet attack on the aliphatic chain.

matic ring. These were also identified in previous works [1,4,8]. Besides, some of the identified TPs resulted from the opening of the aromatic ring due to its breakdown through the HO^\bullet radical consecutive attack on the same carbon atom [8]. Thus, the TP named 182 with m/z 182.1177 was assigned to mono-oxygenated ring opening TP. After the double attack of HO^\bullet on DEET and subsequent ring opening, the decarboxylation involving the loss of CO_2 and H_2O would produce TP 182 [37] whose mono- and dihydroxylation could lead to the formation of TPs 198-A,B,C and 214 (with m/z 198.1129–198.1130 and 214.1072), respectively. On the other hand, ozonolysis of TP 182 could lead to the formation of the TP 146 (m/z 146.0812) through loss of hydrogen peroxide and further HO^\bullet radical attack [18].

Finally, some of the TPs generated could react with ozone and/or hydroxyl radicals to produce short-chain saturated carboxylic acids (oxalic, acetic, pyruvic and formic acids have been detected) which, given their low reactivity towards ozone, eventually would evolve to CO_2 and H_2O by reaction with HO^\bullet (see Scheme 3).

3.5. Kinetic study

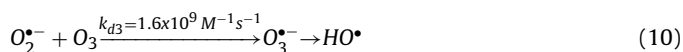
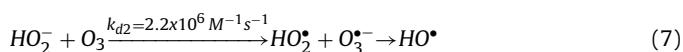
According to the above results, during photocatalytic ozonation DEET degradation and mineralization is mainly due to HO^\bullet radical reactions without a significant direct participation of neither ozone nor positive holes generated on the irradiated photocatalyst surface. Thus, the mechanism of generation of hydroxyl radicals can be described by the following reactions and mass transfer steps:

- Ozone mass transfer from the gas flow to the liquid phase:

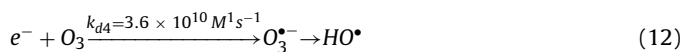
$$\text{O}_{3,g} \xrightarrow{k_{1a} = 5.1 \times 10^{-3} \text{ s}^{-1}} \text{O}_3 \quad (5)$$

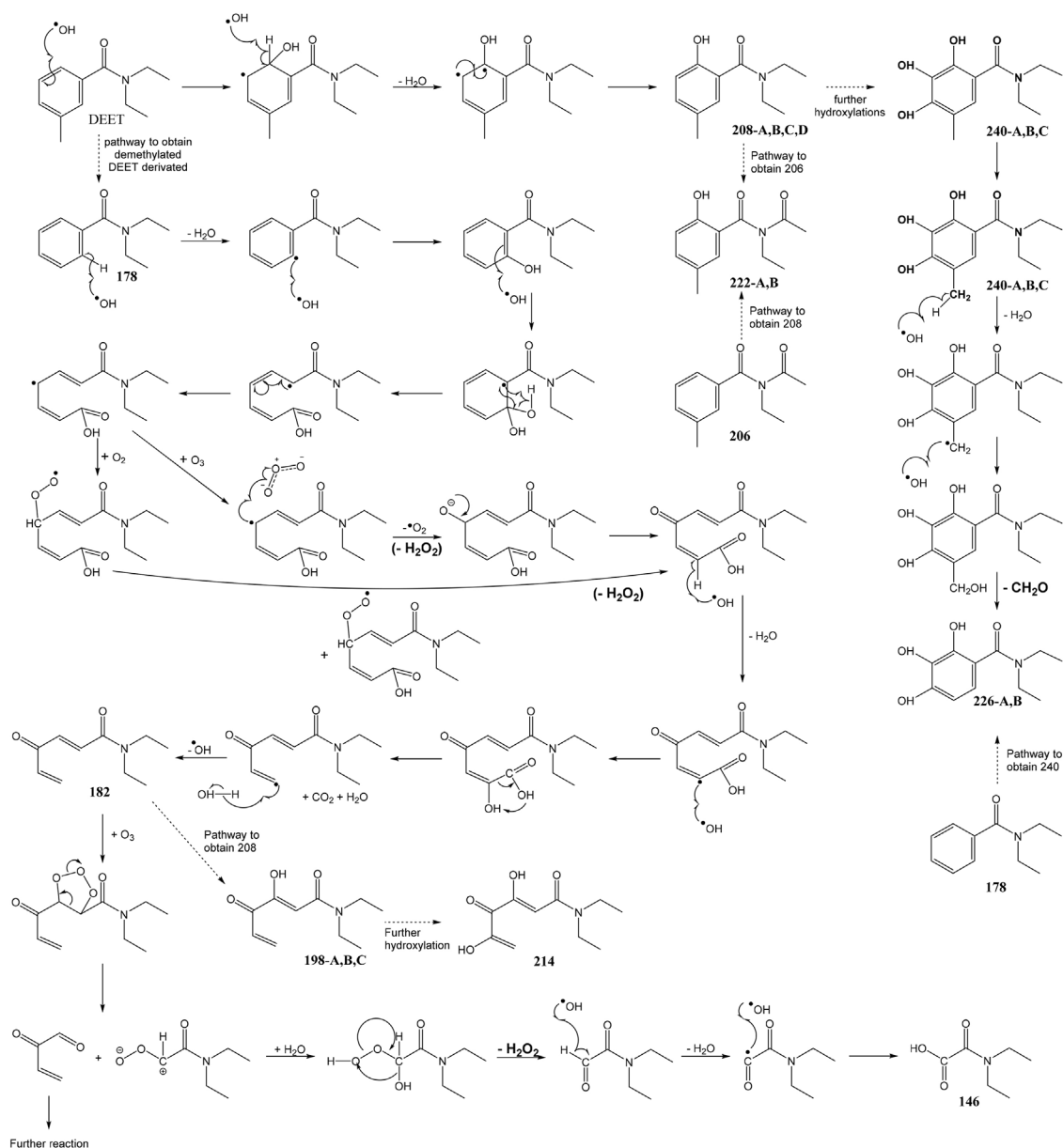
where k_{1a} is the volumetric mass-transfer coefficient that was experimentally determined through O_3 absorption experiments for the reaction system used in this work according to Beltrán in ref. [18].

- Ozone dark decomposition:



- Photocatalytic reactions:



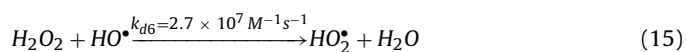
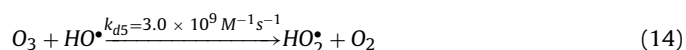


Scheme 2. Proposed DEET degradation pathway through the HO• attack on the aromatic ring.



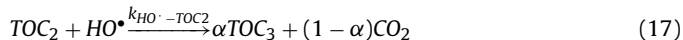
In this mechanism, ozonide radical ($O_3^{\cdot-}$) readily evolves to form hydroxyl radical in Reactions (7), (10) and (12); oxygen is not able to react with photogenerated electrons according to [17], so this reaction has not been taken into account. In addition, although H_2O_2 is decomposed onto irradiated WO_3 surface, the results obtained in terms of DEET degradation and mineralization in experiments conducted by combining PhC- $O_2 + H_2O_2$ (not shown) indicate that no reactive species are formed during H_2O_2 photocatalytic decomposition.

Hydroxyl radicals may react with dissolved ozone and hydrogen peroxide generated according to Reactions (14) and (15):

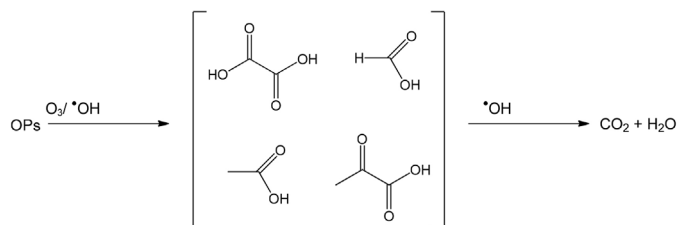


All the known rate constants have been previously summarized in [18]. The rate constant of ozone-electrons reaction has been taken for hydrated electrons from Buxton et al. [31].

In the presence of any organic contaminant at sufficient concentration, hydroxyl radicals will mainly react with it. In terms of TOC, the reaction mechanism of DEET and TOC removal can be described according to the following lumped reactions:



where TOC_1 represents DEET expressed in carbon units; TOC_3 is the total organic carbon corresponding to the sum of short-chain saturated organic acids and formaldehyde in solution detected during photocatalytic ozonation; and TOC_2 is the total organic carbon corresponding to the sum of the rest of DEET intermediates detected by LC-qTOF. In Reaction (17), the stoichiometric parameter α rep-



Scheme 3. Formation of saturated carboxylic acids and mineralization of DEET.

resents the TOC_2 fraction that is converted to TOC_3 whereas $(1-\alpha)$ is mineralized to CO_2 .

TOC_2 can be calculated from the TOC balance:

$$TOC_t = TOC_1 + TOC_2 + TOC_3 \quad (19)$$

where TOC_t is the analyzed total organic carbon in solution at a given time, t .

Mass balances of each species can be established as follows:

- Ozone in the gas phase:

$$v_g C_{O_{3gi}} - v_g C_{O_{3g}} - \beta V k_{la} \left(\frac{C_{O_{3g}} RT}{He} - C_{O_{3d}} \right) = \frac{dC_{O_{3g}}}{dt} (1 - \beta) V \quad (20)$$

where v_g is the gas flow rate; $C_{O_{3gi}}$ and $C_{O_{3g}}$ are the molar ozone concentrations in the gas phase at the reactor inlet and outlet, respectively; $C_{O_{3d}}$ is the molar concentration of dissolved ozone; β is the liquid holdup; V the reaction volume; R the ideal gas constant; and He is the Henry law constant for the ozone-water system at the temperature T .

- Ozone in the liquid phase:

$$\frac{dC_{O_{3d}}}{dt} = \frac{k_{la} C_{O_{3g}} RT}{He} - k_{la} C_{O_{3d}} - k_{d4} C_{O_{3d}} C_{e^-} - k_{d5} C_{O_{3d}} C_{HO^\bullet} \quad (21)$$

where C_{e^-} is the concentration of photogenerated electrons; C_{HO^\bullet} the concentration of hydroxyl radicals; and k_{d4} and k_{d5} the rate constants of Reactions (12) and (14), respectively. In this balance, the contributions of Reactions (6), (7) and (10) have been neglected according to the pH of the reaction medium (from 6 to 4).

- Photogenerated electrons:

$$\frac{dC_{e^-}}{dt} = \phi_{WO_3} I_a^n - k_{d4} C_{O_{3d}} C_{e^-} - k_r C_{h^+} C_{e^-} \quad (22)$$

where ϕ_{WO_3} is the apparent quantum yield of WO_3 at the wavelength range used in this work; I_a is the absorbed radiation flux by the catalyst WO_3 ; the exponent n is the order of the reaction with respect to the I_a and depends on the efficiency of e^-/h^+ formation and recombination at the catalyst surface taking a value between 0.5 and 1 when the reaction is kinetically controlled [38]; C_{h^+} is the concentration of photogenerated holes and k_r is the rate constant of e^-/h^+ recombination Reaction (13). If ozone concentration is high enough, the recombination process is minimized so it can be considered that all the photogenerated electrons are trapped by dissolved ozone. Then Eq. (22) can be simplified as:

$$\frac{dC_{e^-}}{dt} = \phi_{WO_3} I_a^n - k_{d4} C_{O_{3d}} C_{e^-} \quad (23)$$

- Hydroxyl radicals:

$$\begin{aligned} \frac{dC_{HO^\bullet}}{dt} = & k_{d4} C_{O_{3d}} C_{e^-} - k_{d5} C_{O_{3d}} C_{HO^\bullet} - k_{d6} C_{H_2O_2} C_{HO^\bullet} \\ & - k_{HO^\bullet-TOC1} C_{TOC1} C_{HO^\bullet} - \\ & - k_{HO^\bullet-TOC2} C_{TOC2} C_{HO^\bullet} - k_{HO^\bullet-TOC3} C_{TOC3} C_{HO^\bullet} \end{aligned} \quad (24)$$

where $C_{H_2O_2}$ is the concentration of hydrogen peroxide in the liquid phase; C_{TOC1} , C_{TOC2} and C_{TOC3} are the concentrations corresponding to TOC_1 , TOC_2 and TOC_3 , respectively; and k_{d6} , $k_{HO^\bullet-TOC1}$, $k_{HO^\bullet-TOC2}$, $k_{HO^\bullet-TOC3}$ are the rate constants of Reactions (15), (16), (17) and (18), respectively.

Eq. (24) can be rewritten as follows:

$$\frac{dC_{HO^\bullet}}{dt} = k_{d4} C_{O_{3d}} C_{e^-} - C_{HO^\bullet} \sum_i k_i C_i \quad (25)$$

where the subscript i represents any species that reacts with hydroxyl radicals.

For Eq. (23) and (25), net reaction rates were assumed to be zero according to the hypothesis of the stationary state for transient species. Thus, hydroxyl radical concentration can be expressed as follows:

$$C_{HO^\bullet} = \frac{\phi_{WO_3} I_a^n}{\sum_i k_i C_i} = \frac{r_i}{k_s} \quad (26)$$

In Eq. (26) the numerator r_i represents the reaction rate of initiation for the formation of hydroxyl radicals, whereas the denominator k_s represents the scavenging factor, taking into account that the species involved in this term are only the inhibitors of the chain mechanism of ozone decomposition into HO^\bullet .

- Total organic carbon mass balances:

$$\frac{dC_{TOC1}}{dt} = -k_{HO^\bullet-TOC1} C_{TOC1} C_{HO^\bullet} = -k_{HO^\bullet-TOC1} C_{TOC1} \frac{r_i}{k_s} \quad (27)$$

$$\begin{aligned} \frac{dC_{TOC2}}{dt} = & k_{HO^\bullet-TOC1} C_{TOC1} C_{HO^\bullet} - k_{HO^\bullet-TOC2} C_{TOC2} C_{HO^\bullet} = \\ & = (k_{HO^\bullet-TOC1} C_{TOC1} - k_{HO^\bullet-TOC2} C_{TOC2}) \frac{r_i}{k_s} \end{aligned} \quad (28)$$

$$\begin{aligned} \frac{dC_{TOC3}}{dt} = & \alpha k_{HO^\bullet-TOC2} C_{TOC2} C_{HO^\bullet} - k_{HO^\bullet-TOC3} C_{TOC3} C_{HO^\bullet} = \\ & = (\alpha k_{HO^\bullet-TOC2} C_{TOC2} - k_{HO^\bullet-TOC3} C_{TOC3}) \frac{r_i}{k_s} \end{aligned} \quad (29)$$

where $k_{HO^\bullet-TOC1}$ is the rate constant of DEET- HO^\bullet reaction; $k_{HO^\bullet-TOC2}$ represents the apparent rate constant of the reaction between TOC_2 (DEET intermediates detected by LC-qTOF) and HO^\bullet radicals; and $k_{HO^\bullet-TOC3}$ represent an apparent rate constant of the reaction between compounds of TOC_3 (formaldehyde and oxalic, acetic, pyruvic and formic acids) and HO^\bullet .

Firstly, the hypothesis of working in excess of ozone was proved by means of two different experiments with different ozone concentration at the reactor inlet (10 and 20 mg L⁻¹). Results of DEET degradation and mineralization are represented in Fig. 9(A) where it can be noticed the similar evolution of DEET and TOC regardless of the ozone concentration used.

Thus, to solve the proposed model for TOC evolution, the initiation rate r_i was determined in an experiment of photocatalytic ozonation of pCBA in the presence of oxalic acid. In this system, pCBA is a HO^\bullet probe which has very low reactivity with ozone but readily reacts with HO^\bullet (see rate constants in Table 1) [39]. Oxalic acid was used in this experiment at high concentration as HO^\bullet scav-

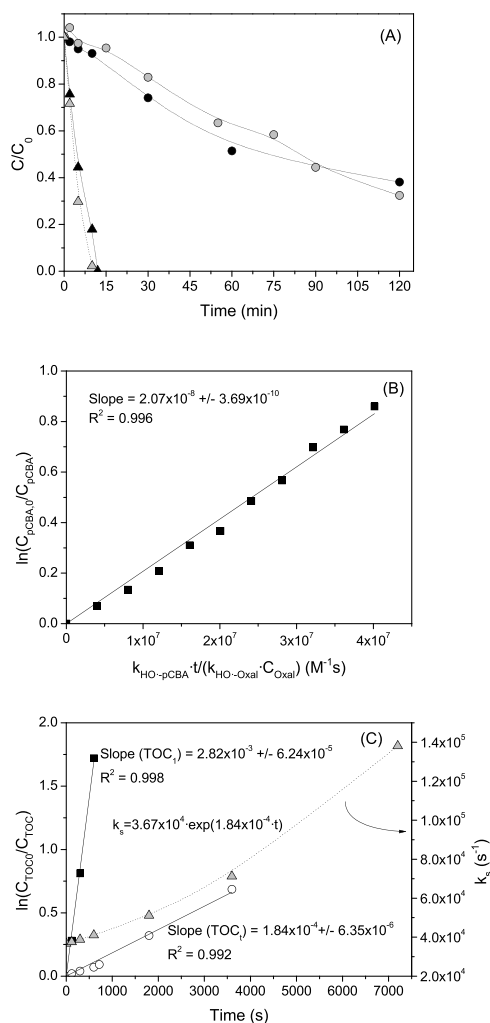


Fig. 9. Determination of kinetic parameters. (A) Time evolution of DEET (triangles) and TOC (circles) normalized concentrations during PhC-O₃ at different O₃ inlet gas concentration. Symbols: ●, ▲ 10 mg L⁻¹; ●, ▲ 20 mg L⁻¹. (B) *r_i* determination from pCBA-oxalic acid experiment through data fitting to Eq. (32). (C) *k_s* determination from TOC evolution. Symbols: ■ TOC₁ (line shows fitting of Eq. (33)); ° TOC₂ (line shows fitting to apparent 1st order kinetics); ▲ *k_s*. Experimental conditions: C_{DEET,0} = 15 mg L⁻¹; pH₀ = 6; V = 0.5 L; Q_g = 15 L h⁻¹; CO_{3,g} = 10 mg L⁻¹; I = 550 W m⁻²; *C_{WO3} = 0.25 g L⁻¹; *C_{pCBA,0} = 5 mg L⁻¹; *C_{Oxal,0} = 0.01 M (*if applied).

enger. Thus, in the presence of both compounds, the evolution of pCBA can be expressed as:

$$\frac{dC_{pCBA}}{dt} = -k_{HO\cdot-pCBA}C_{pCBA}C_{HO\cdot} = -k_{HO\cdot-pCBA}C_{pCBA}\frac{r_i}{k_s} = -k_{HO\cdot-pCBA}C_{pCBA}\frac{r_i}{k_{HO\cdot-Oxal}C_{Oxal}} \quad (30)$$

where C_{pCBA} and C_{Oxal} are the concentrations of pCBA and oxalic acid, respectively; $k_{HO\cdot-pCBA}$ and $k_{HO\cdot-Oxal}$ are the rate constants in Table 1 ($k_{HO\cdot-Oxal} = 4.6 \times 10^6 \text{ M}^{-1} \text{ s}^{-1}$, at pH = 4). In this equation, oxalic acid is considered as an inhibitor of the chain mechanism of ozone decomposition into HO• radicals [40]. Integration of Eq. (30) leads to Eq. (31) which simplifies to Eq. (32) since oxalic acid remains virtually constant while pCBA is depleted and r_i will be constant at the conditions used:

$$\ln \frac{C_{pCBA,0}}{C_{pCBA}} = \frac{k_{HO\cdot-pCBA}}{k_{HO\cdot-Oxal}} \int_{t_0}^t \frac{r_i}{C_{Oxal}} dt \quad (31)$$

Table 4

Kinetic parameters and correlation coefficient of the model proposed for PhC-O₃ DEET mineralization.

Parameter	Value
$r_i \text{ (M s}^{-1}\text{)}$	2.07×10^{-8}
$k_{HO\cdot-TOC1} \text{ (M}^{-1} \text{ s}^{-1}\text{)}$	5×10^9
$k_{HO\cdot-TOC2} \text{ (M}^{-1} \text{ s}^{-1}\text{)}$	1.3×10^9
$k_{HO\cdot-TOC3} \text{ (M}^{-1} \text{ s}^{-1}\text{)}$	4×10^8
α	0.62
R^2	0.993

$$\ln \frac{C_{pCBA,0}}{C_{pCBA}} = \frac{k_{HO\cdot-pCBA}}{k_{HO\cdot-Oxal} \cdot C_{Oxal}} r_i t \quad (32)$$

The representation of Eq. (32) is depicted in Fig. 9(B), and the calculated value for r_i is indicated in Table 4.

During photocatalytic ozonation of DEET, the scavenging factor, k_s could not be considered constant. This scavenging factor will involve all the species reacting with hydroxyl radicals that inhibit the ozone decomposition mechanism. During the first moments, when DEET concentration is high and no mineralization is observed, k_s can be determined from integrated Eq. (27):

$$\ln \frac{C_{TOC10}}{C_{TOC1}} = k_{HO\cdot-TOC1} \frac{r_i}{k_s} t \quad (33)$$

As observed in Fig. 9(C), k_s was found to be $3.67 \times 10^4 \text{ s}^{-1}$ (for the initial moments of reaction) from plotting and fitting experimental data to Eq. (33). However, since the composition of the reaction medium changes with time, this k_s value is not valid for the entire reaction period. In general, as reaction progresses, the concentration of organic intermediates with inhibiting character such as oxalic or acetic acid increase. Thus, taking into account that the main organics involved in the scavenging factor are constituents of TOC_t, an approximation was done taking into account that k_s undergoes an exponential variation with time inversely to TOC_t, at $t=0$ being $k_{s0} = 3.67 \times 10^4 \text{ s}^{-1}$, as calculated for the beginning of the experiment. The evolution of $\ln(C_{TOC,0}/C_{TOC})$ and k_s with time is depicted in Fig. 9(C), the selected fitting equation for k_s being:

$$k_s = 3.67 \times 10^4 \exp(1.84 \times 10^{-4} t) \quad (34)$$

With all these calculated data, differential Eqs. (27)–(29) can be simultaneously solved. For that purpose, $k_{HO\cdot-TOC3}$ apparent rate constant of the reaction between compounds of TOC₃ (formaldehyde and oxalic, acetic, pyruvic and formic acids) and HO• radicals, has been calculated as an average value taking into account their individual rate constants [31]. Values of $k_{HO\cdot-TOC1}$ and $k_{HO\cdot-TOC3}$ are summarized in Table 4. The other values, $k_{HO\cdot-TOC2}$ and α , were used as fitting parameters to minimize the difference between experimental data and those calculated with the proposed model. The resolution of the differential equations was performed by a fourth-order Runge-Kutta method with Micromath Scientist 3.0 software. Fig. 10 shows the experimental and calculated TOC evolution. As observed, the proposed kinetic model fits fairly well the experimental results (also confirmed by the R^2 value in Table 4). In addition, as expected, for the reaction between TOC₂ and HO• radicals the value of the rate constant obtained ($k_{HO\cdot-TOC2}$) is lower than that of DEET-HO• reaction but higher than that of TOC₃-HO•, which is in accordance with the general trend of subsequent lower reactivity of the OPs formed in these type of reactions [31]. On the other hand, 62% of the TOC₂ is transformed in TOC₃ whereas 38% can be mineralized according to the apparent stoichiometric coefficient α .

The proposed kinetic model provides a simplified approach that can be useful for design purposes, although the nature of the organic pollutant and its reactivity with the different oxidizing species generated during photocatalytic ozonation, together with the operating conditions, will play an important role in order to extend

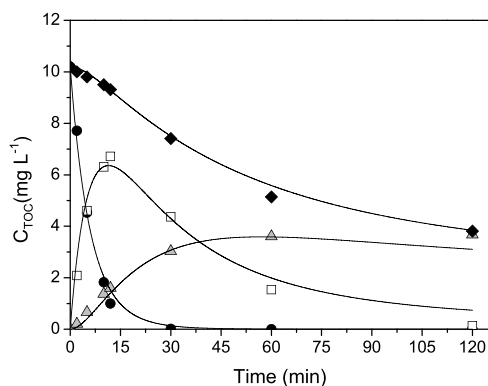


Fig. 10. Evolution of TOC with time during DEET degradation by PhC-O₃. Symbols: ♦ TOC_t; ● TOC₁ (DEET); □ TOC₂ (OPs); ▲ TOC₃ (Carboxylic acids and formaldehyde); lines are fitting results from the TOC depletion model. Experimental conditions: C_{DEET,0} = 15 mg L⁻¹; pH₀ = 6; V = 0.5 L; Q_g = 15 L h⁻¹; C_{O_{3,g}} = 10 mg L⁻¹; I = 550 W m⁻²; C_{WO₃} = 0.25 g L⁻¹.

the model from this particular case to more general photocatalytic ozonation studies.

4. Conclusions

A synergistic effect between ozone and visible light irradiated WO₃ has been proved. The highest efficiency of photocatalytic ozonation process compared to photocatalysis and single ozonation is reflected in both, DEET depletion and mineralization rates, hydroxyl radicals in the bulk being the main species responsible according to scavenging experiments. At the conditions used in this work, photocatalytic ozonation process led to complete removal of 15 mg L⁻¹ DEET in 15 min with mineralization up to 60% in 2 h. The detailed study of the evolution with time of 22 TPs detected during ozonation and photocatalytic ozonation allowed the proposal of a general reaction mechanism through different pathways mainly based on the hydroxyl radical attack. The reaction mechanism involves steps of mono- and poly-hydroxylation and/or oxidation, de-alkylation and finally opening of the aromatic ring which evolves through further oxidation, to the formation of short-chain saturated organic acids and mineralization to CO₂. The evolution of DEET, intermediates and short-chain saturated organic acids was fitted to a lumped kinetic model based on TOC-hydroxyl radical reactions and provides a simplified approach for this process that can be useful for design purposes. However, the nature of the organic pollutant and its reactivity towards the different reactive species generated during photocatalytic ozonation (ozone, hydroxyl radicals, positive holes, etc.); as well as the operating conditions (pH, temperature, radiation intensity and wavelength, etc.) would play an important role in order to extend the model from this particular case and will be considered for a future work.

Acknowledgements

Authors thank the Spanish MINECO and European Feder Funds (CTQ2015/64944-R) and Junta de Extremadura (Ayuda a Grupos Exp. GR15-033) for economic support; and SAEM-SAIUEX for

the LC-qTOF analyses. E. Mena thanks the Consejería de Empleo, Empresa e Innovación (Junta de Extremadura) and European Social Fund for her FPI grant (Ref. PD12059).

References

- [1] M. Antonopoulou, A. Giannakas, Y. Deligiannakis, I. Konstantinou, *Chem. Eng. J.* 231 (2013) 314–325.
- [2] S.D. Costanzo, A.J. Watkinson, E.J. Murby, D.W. Kolpin, M.W. Sandstrom, *Sci. Total Environ.* 384 (2007) 214–220.
- [3] W.A. Adams, C.A. Impellitteri, *J. Photochem. Photobiol. A Chem.* 202 (2009) 28–32.
- [4] F.J. Benítez, J.L. Acero, J.F. García-Reyes, F.J. Real, G. Roldán, E. Rodríguez, A. Molina-Díaz, *Ind. Eng. Chem. Res.* 52 (2013) 17054–17073.
- [5] N. Petrucci, S. Sardini, *Pediatr. Emerg. Care* 16 (2000) 341–342.
- [6] F.J. Benítez, J.L. Acero, F.J. Real, G. Roldán, E. Rodríguez, *Ozone Sci. Eng.* 35 (2013) 263–272.
- [7] W. Li, V. Nanaboina, Q. Zhou, G.V. Korshin, *Water Res.* 46 (2012) 403–412.
- [8] C. Medana, P. Calza, F. Dal Bello, E. Raso, C. Minero, C. Baiocchi, *J. Mass Spectrom.* 46 (2011) 24–40.
- [9] E. Mena, A. Rey, B. Acedo, F.J. Beltrán, S. Malato, *Chem. Eng. J.* 204–206 (2012) 131–140.
- [10] T.E. Agustina, H.M. Ang, V.K. Vareek, *J. Photochem. Photobiol. C Photochem. Rev.* 6 (2005) 264–273.
- [11] E. Mena, A. Rey, F.J. Beltrán, S. Contreras, *Catal. Today* 252 (2015) 100–106.
- [12] K.S. Tay, N. Abd Rahman, M.R. Bin Abas, *Chemosphere* 76 (2009) 1296–1302.
- [13] H. Bader, J. Hoigné, *Water Res.* 15 (1981) 449–456.
- [14] I. Ilisz, A. Bokros, A. Dombi, *Ozone Sci. Eng.* 26 (2004) 585–594.
- [15] W. Masschelein, M. Denis, R. Ledent, *Water Sewage Works (August)* (1977) 69–72.
- [16] R. Flyunt, A. Leitzke, G. Mark, E. Mvula, E. Reisz, R. Schick, C. von Sonntag, *J. Phys. Chem. B* 107 (30) (2003) 7242–7253.
- [17] S. Nishimoto, T. Mano, Y. Kameshima, M. Miyake, *Chem. Phys. Lett.* 500 (2010) 86–89.
- [18] F.J. Beltrán, *Ozone Reaction Kinetics for Water and Wastewater Systems*, Boca Raton, CRC Press, Florida, USA, 2004.
- [19] L. Sánchez, X. Domènech, J. Casado, J. Peral, *Chemosphere* 50 (2003) 1085–1093.
- [20] D.H. Quiñones, A. Rey, P.M. Álvarez, F.J. Beltrán, P.K. Plucinski, *Appl. Catal. B Environ.* 144 (2014) 96–106.
- [21] W. Song, W.J. Cooper, B.M. Peake, S.P. Mezyk, M.G. Nickelsen, K.E. O'shea, *Water Res.* 43 (3) (2009) 635–642.
- [22] C.C.D. Yao, W.R. Haag, *Water Res.* 25 (1991) 761–773.
- [23] M.S. Alam, B.S.M. Rao, E. Janata, *Radiat. Phys. Chem.* 67 (2003) 723–728.
- [24] P.N. Johnson, R.A. Davis, *J. Chem. Eng. Data* 41 (1996) 1485–1487.
- [25] G.F. Froment, K.B. Bischoff, *Chemical Reactors Analysis and Design*, John Wiley & Sons, New York, USA, 1979.
- [26] S. Staehelin, J. Hoigné, *Environ. Sci. Technol.* 16 (1982) 666–681.
- [27] F.J. Beltrán, A. Aguinaco, J.F. García-Araya, *Water Res.* 43 (2009) 1359–1369.
- [28] L.S. Zhang, K.H. Wong, D.Q. Zhang, C. Hu, J.C. Yu, C.Y. Chan, P.K. Wong, *Environ. Sci. Technol.* 43 (2009) 7883–7888.
- [29] E.M. Rodríguez, G. Márquez, M. Tena, P.M. Álvarez, F.J. Beltrán, *Appl. Catal. B Environ.* 178 (2015) 44–53.
- [30] J. Hoigné, H. Bader, *Water Res.* 17 (1983) 185–194.
- [31] G.V. Buxton, C.L. Greenstock, W.P. Helman, J. Phys. Chem. Ref. Data 17 (1988) 513–886.
- [32] A.D. Coelho, C. Sans, A. Agüera, M.J. Gomez, S. Esplugas, M. Dezotti, *Sci. Total Environ.* 407 (2009) 3572–3578.
- [33] H. Zhang, A.T. Lemley, *Environ. Sci. Technol.* 40 (2006) 4488–4494.
- [34] P. Calza, C. Medana, E. Raso, V. Giannotti, C. Minero, *Sci. Total Environ.* 409 (2011) 3894–3901.
- [35] A. Leitzke, C. von Sonntag, *Ozone Sci. Eng.* 31 (2009) 301–308.
- [36] A. Aguinaco, F.J. Beltrán, J.P. Sagasti, O. Gimeno, *Chem. Eng. J.* 235 (2014) 46–51.
- [37] F.J. Beltrán, O. Gimeno, F.J. Rivas, M. Carbajo, *J. Chem. Technol. Biotechnol.* 81 (2006) 1787–1796.
- [38] S. Malato, P. Fernández-Ibáñez, M.I. Maldonado, J. Blanco, W. Gernjak, *Catal. Today* 147 (2009) 1–59.
- [39] M.S. Elovitz, U. von Gunten, *Ozone Sci. Eng.* 21 (1999) 239–260.
- [40] N.K.V. Leitner, M. Doré, *Water Res.* 31 (1997) 1383–1397.